CONF-890661--4

UCRL-98804
PREPRINT

# Capabilities and Some Applications of the LLNL 100-kV Electric Gun



J. E. Osher
G. R. Gathers
H. H. Chau
R. C. Weingart

This paper was prepared for the Third High Dynamic Pressures Symposium
June 5–9, 1989, La Grande Motte, France

June 5, 1989

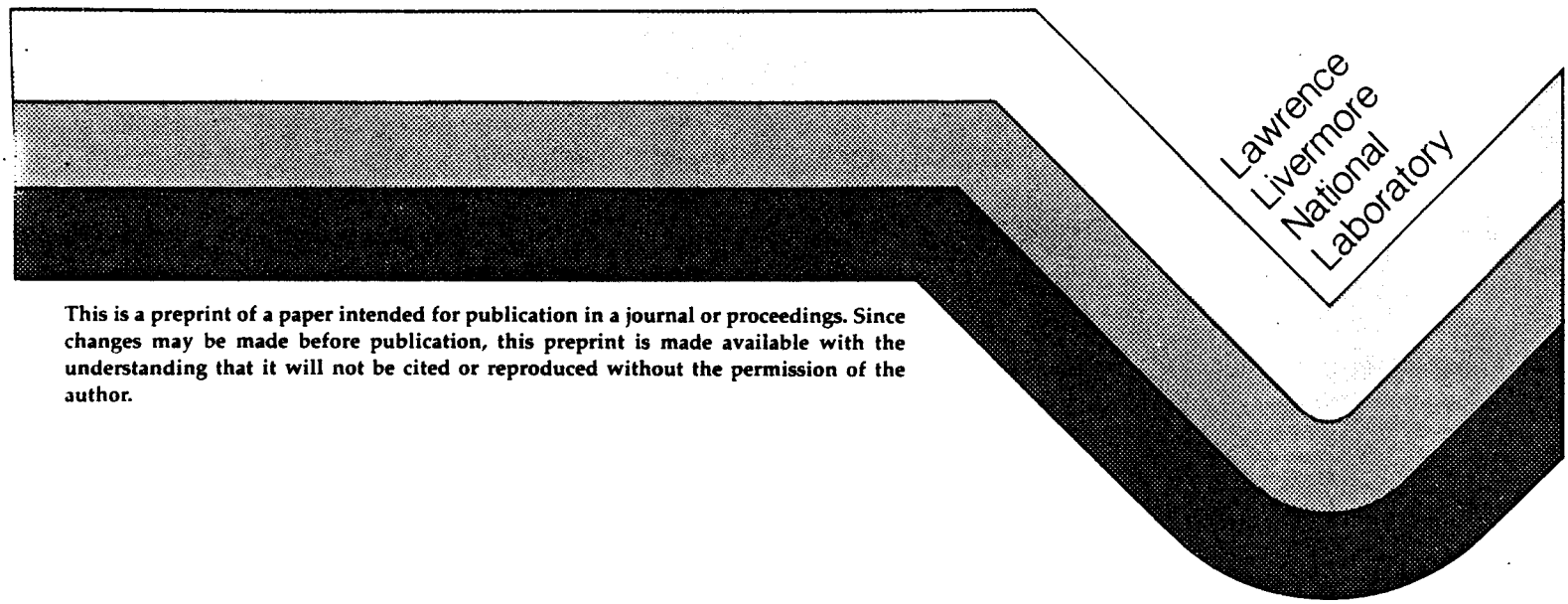

---

# Capabilities and Some Applications of the LLNL 100-kV Electric Gun

J.E. Osher, G.R. Gathers, H.H. Chau, and R.C. Weingart

Lawrence Livermore National Laboratory
P.O. Box 808
Livermore, CA 94551

UCRL--98804

DE89 006747

## Abstract

The LLNL 100-kV electric gun is an experimental device for launching thin flyer plates at velocities as high as 20 km/s to study impact damage and shock-wave physics. The hypervelocity impact studies reported here include a damage study of spalling damage in aluminum, a study of one-dimensional shock-wave attenuation in materials, use of the well-characterized one-dimensional shock waves for equation-of-state measurements in various materials, and use of thin flyer plates at velocities up to 18 km/s to produce reverse ballistic impact on target objects such as rods to measure damage and fragmentation. Our studies include both experimental results and correlation with numerical calculations using a code such as DYNA2D.

## I. Introduction

The electric gun uses the energy initially stored in a capacitor bank to ohmically heat and explode a thin metal bridge-foil (BF) load element. The BF load is mounted on top of a disposable, one-shot, low-inductance, parallel-plate transmission-line "laminate." A cover layer of dielectric is bonded over the top of the BF and transmission lines.

For operation, a disposable (one-shot) gun barrel is aligned over the BF element and bonded to the cover layer of the laminate. The gun-barrel bore serves to cut out the flyer from the cover layer, and the barrel material serves as tamping to minimize side expansion during the BF plasma expansion phase that accelerates the flyer up the barrel. The electrical circuit that powers the BF load is a simple resistance-inductance-capacitance circuit, but the BF acts as a very nonlinear resistive element as it is rapidly heated through the vapor phase during the explosion. Figure 1 shows an exploded view of the gun-laminate components, the diagnostic arrangement for a typical spall experiment, and the gun circuit.

The characteristics of the 100-kV capacitor bank that supplies power to the electric gun have been previously described [1,2]; briefly, the maximum energy available from the 17.3-μF bank at 100 kV is 87 kJ, and the rise time (quarter period) of the current is just over 1.0 μs. The circuit inductance of approximately 26 nH allows a maximum $dI/dt = 4 \times 10^{12}$ A/s.

This work was performed under the auspices of the U.S. Department of Energy by the Lawrence Livermore National Laboratory under Contract W-7405-Eng-48.

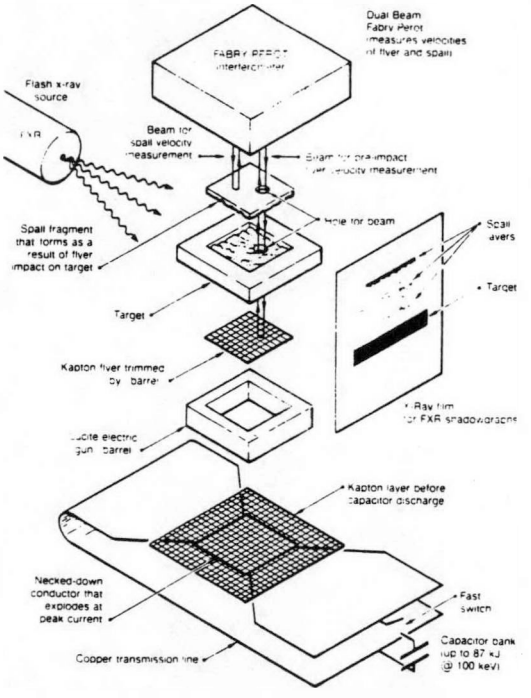


**Figure 1. Setup for electric-gun and flyer-plate experiments illustrating the key events and diagnostics involved in a typical spallation experiment.**

## II. Diagnostics and Flyer Characteristics

The environment of the gun laminate during flyer acceleration contains currents in the MA range and the possibility of substantial electromagnetic interference (EMI), so optical diagnostics are preferred. The principal diagnostic instrument for measuring the velocity of the flyer is a dual-beam Fabry-Perot (F-P) velocimeter [3]. The instrument measures the doppler shift of an argon-ion laser beam reflected from a thin aluminized spot on the surface of the flyer (or other selected surface). This technique allows continuous, precise (less than ±1% error) measurement of velocity. The split- or dual-beam feature allows simultaneous measurement of the velocity of a secondary surface such as a spall scab produced by impact damage.

Another diagnostic for evaluating flyer performance is an electronic streaking camera. The camera records the light over a moving slit image (through suitably transparent materials). The light flash produced when the flyer strikes a surface can be observed to measure impact times, to assess two-dimensional flatness of the flyer at impact, or, with a suitable step flasher, to measure the average flyer speed. Figure 2 shows a recorded sequence produced by the impact of a 7.62-mm-diameter, 0.254-mm-thick Teflon flyer at 10.5 km/s on a glass witness plate. First visible is the impact flash, then a brief cutoff of light by the damaged witness plate, and finally late light emitted by the hot aluminum plasma leaking through the debris. The deviation from flatness over the main portion of the diameter is less than 9 mrad.

The third major diagnostic is a dual-head flash x-ray system used to study the kinematics of impact debris at selected times. The gun's containment vessel is operated at atmospheric pressure, but the BF load and muzzle-target region of the gun can be operated under vacuum using an appropriate (one-shot) vacuum fixture. The target is generally recovered in a foam catcher with minimal secondary damage (since a large fraction of the energy in the system is in the form of kinetic energy of the thin flyer).

The end result is a system capable of accelerating relatively thick, large-area flyers to velocities in the range of up to 4 km/s and thin, small-area flyers up to 20 km/s. Specifically, a 0.3-mm-thick Kapton flyer with an area of 100 $cm^2$, weighing 4.3 g, can be accelerated to 3.2 km/s. This represents some 22 kJ of kinetic energy (from the original 87 kJ in the bank) for a conversion efficiency of 25% from stored electrical energy to kinetic energy. At the other extreme, the system can accelerate a 1-$cm^2$ flyer of 0.3-mm-thick Kapton, weighing 43 mg, to 18 km/s, or some 7 kJ, for an energy conversion efficiency of 8%. Thinner flyers can be accelerated to still higher velocities, but their integrity at impact is not well defined.

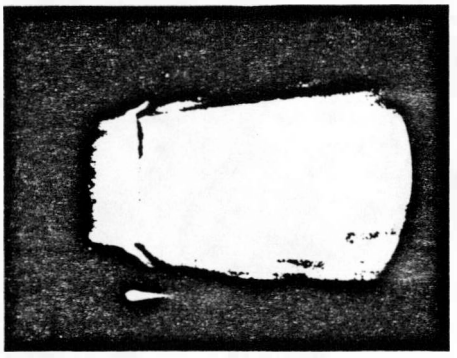

**Figure 2. Streak-camera record of the light flash generated by a 7.6-mm-diameter, 0.254-mm-thick Teflon flyer impacting a glass target at 10.5 km/s. Time runs from left to right, with the fiducial time marker about 100 ns long.**

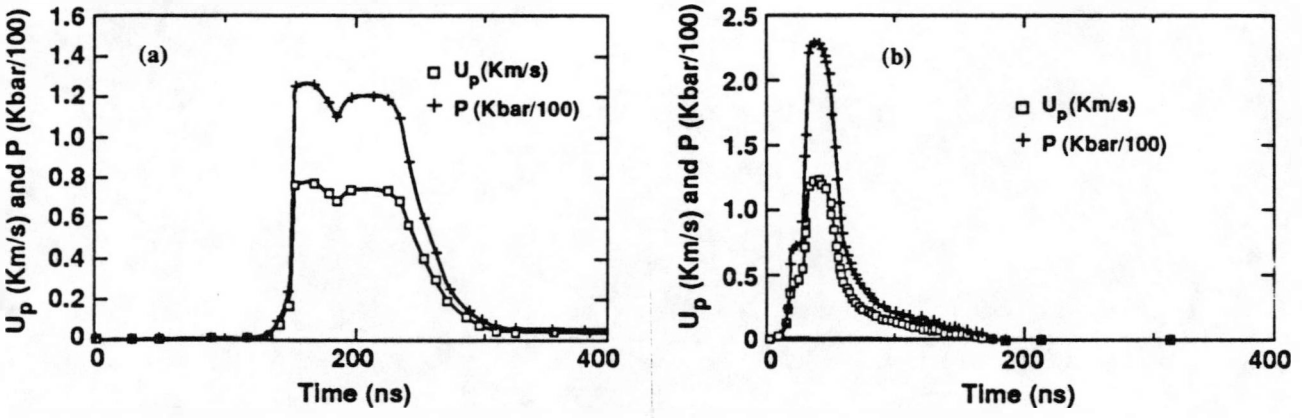


**Figure 3. Typical one-dimensional pulse shapes produced by Kapton flyer impacting on aluminum or LiF targets. (a) Particle jump-off velocity, $U_p$, measured at the Al/LiF interface for a 0.3-mm-thick Kapton flyer at 2.4 km/s incident on a diagnostic target. The pressure pulse shown is derived from the measured value of $U_p$ and the known Hugoniot for LiF. (b) Corresponding data for a 0.1-mm-thick Kapton flyer impacting a similar diagnostic target at 4.0 km/s.**

An example of the one-dimensional pressure pulses available for shock-wave studies is shown in Fig. 3. A 0.3-mm-thick Kapton flyer accelerated to 2.4 km/s impacted a diagnostic target composed of a 0.075-mm-thick aluminum foil bonded to a 5-mm-thick lithium fluoride (LiF) crystal with a thin film of mineral oil. Figure 4a shows the mass velocity, $U_p$, of the interface between the aluminum and the LiF. From the known Hugoniot in the LiF and the measured jump-off particle velocity, $U_p$, at the Al/LiF interface, one can calculate the pressure pulse in the LiF. The slight notch in the measured $U_p$ and the deduced pressure of up to 13 GPa (130 kbar) are due to the fact that our "0.3-mm-thick Kapton" flyer is actually made up of two pieces, each of 0.127-mm-thick Kapton plus a layer of 0.025-mm-thick adhesive. Figure 4b shows the corresponding particle velocity and derived pressure of up to 23 GPa (230 kbar) for a 0.1-mm-thick Kapton flyer (actually 0.075 mm of Kapton plus 0.025 mm of adhesive) striking a similar diagnostic target at 4 km/s. The 100-ns and 30-ns duration of the pulses, respectively, is just the reverberation time of the shock waves in the flyer material.

## III. Hypervelocity Impact Applications

### Spalling and Impact-Gain Studies

The electric gun can be used to generate strong, short-duration, one-dimensional shock waves (up to several hundreds of GPa or several Mbar). Among other applications, such shock waves can be used either in basic material damage studies or to simulate the effects of cosmic debris impacting on appropriately scaled space systems. We present here the specific case of spalling damage to illustrate the damage application.

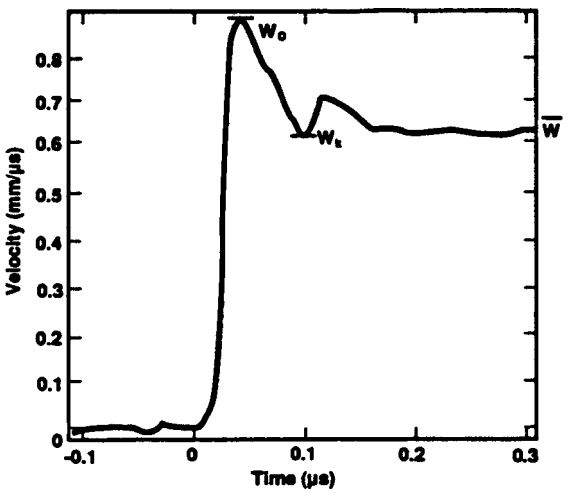


**Figure 4. F-P trace of the velocity of the first (top) spall scab produced by impact of a 0.1-mm-thick Kapton flyer at 4.0 km/s on a target of 3.17-mm-thick 6061-T6 aluminum.**

When a triangular-shaped or very-short-duration shock wave reaches a free surface, the reflected rarefaction wave (required to satisfy the zero pressure condition on the free surface) interacts with the tail of the incident wave, resulting in tensile stress within the material. If the tensile stress exceeds the strength of the material, the material ruptures or spalls, producing a new free surface and a new region of tensile stress that can cause another spall, the process repeating (as multiple spallation) until the tensile stress level in the material finally drops below the stress threshold for for spall failure.

Electric-gun spalling studies include a well-calibrated incident pulse and recovery of the remnant target and the free spall scab (if present). References [1] and [4] briefly survey the threshold for spalling of 6061-T6 aluminum with pulses of both 100 ns and 30 ns duration. There we note that the threshold for spalling damage is not a sharply defined stress level. At incident pulse levels well below the generally accepted threshold level, damage shows up in the formation of a very thin layer of microvoids. At a level near but still below threshold, damage takes the form of of incipient spall blisters. At a level just above the threshold for free spalling, we observe a single, relatively thick spall-scab layer coming off, and at higher impulse levels we observe formation of multiple thin layers of spall.

The dual-beam F-P diagnostic allows measuring both the velocity of the flyer and that of the top surface of the first spall scab. The measured difference in velocity of the top surface of the spall scab, between the initial peak velocity upon arrival of the shock front and the first minimum in the pull-back velocity (due to inertia of the rest of the material in the target) before rupture, allows calculation of the critical threshold stress level for free spalling failure of the target material. In the notation of Novikov and Chernov [5] the spall strength, $\sigma_0$, for this case is

$$\sigma_0 = \rho_0 \times C_0 \times (W_0 - W_k)/2 \qquad (1)$$

$$\sigma_0 = \rho_0 \times C_0 \times (W_0 - \overline{W}), \qquad (2)$$

where $\rho_0$ is the initial density, $C_0$ is the sound speed, $W_0$ is the initial peak spall-scab velocity, $W_k$ is the first minimum in the pull-back to rupture, and $\overline{W}$ is the final average spall-scab velocity.

Figure 4 shows the F-P trace of the velocity of the top spall scab for a 0.1-mm-thick Kapton flyer incident at 4.0 km/s on a target of 3.17-mm-thick 6061-T6 aluminum. In this case we obtain a spall strength, $\sigma_0$, of about 1.7 GPa (17 kbar) for the 6061-T6 aluminum. The results of an early survey of the threshold for spall and use of this technique for measuring the spall strength of materials is reported by Froeschner et al. [6].

The next diagnostic used in the study of spallation was the flash x-ray unit. The arrangement of the x-ray tube and film cassette is shown in Fig. 1, together with a representation of typical spalling data. Figure 5 shows a classic example of the multiple spall layers observed for a flyer impacting on 6061-T6 aluminum. The radiograph of the spall layers and the target remnant are shown in Fig. 5a, and a densitometer scan in the midplane of the radiograph is plotted as the log of the transmitted x-ray intensity in Fig. 5b. The radiograph for this case was taken 30 μs after impact of a 0.3-mm-thick

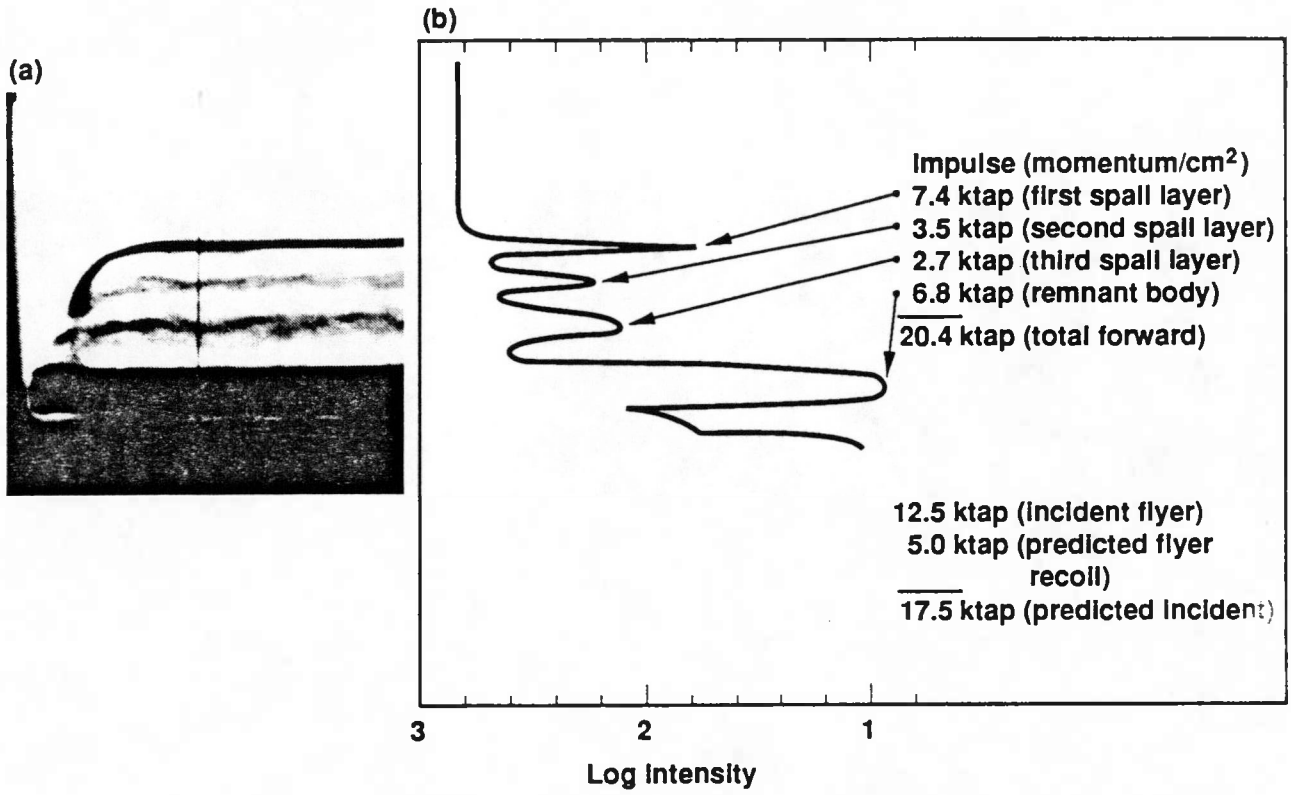


**Figure 5. (a) Flash x-ray image taken 30 μs after impact of a 0.3-mm-thick Kapton flyer at 2.9 km/s on a 6.35-mm-thick target of 6061-T6 aluminum. (b) Densitometer readout (logarithm of the x-ray intensity transmitted through the debris to the x-ray film) averaged over a central strip of the image. The notation to the right shows the momenta in ktap for each portion of the debris.**

Kapton flyer at 2.9 km/s on a 76.2-mm-by-76.2-mm sample of 6.35-mm-thick 6061-T6 aluminum. The recovered specimen allows measuring the total mass loss in all the spall layers to normalize the relative densitometer trace. The mass in each spall layer, and its velocity deduced from the observed displacement on the x-ray radiograph (from its initial position in a set-up radiograph), allow calculation of the momentum in each fragment as shown in the inserts of Fig. 5b. The end result is an apparent impulse gain of just over 1.6 times the incident flyer impulse of 12.5 ktap (impulse/cm$^2$ is given here in taps, with units of areal density in g/cm$^2$ times the flyer velocity in cm/s).

The gain in impulse over the incident impulse is not unexpected, since the light Kapton flyer recoils from the more dense aluminum target. The predicted recoil for this case, calculated using the principal Hugoniot for the Kapton as an approximation to the release isentrope, yields a recoil Kapton momentum of about 5.0 ktap. The measured gain (the ratio of the final total forward momentum to the initial incident flyer momentum) thus exceeds the predicted impulse gain. Figure 6 shows the results of a brief survey of the measured and "predicted" impulse gain for the case of 0.3-mm-thick Kapton flyers impacting at velocities from 0.68 km/s to 3.55 km/s on various thicknesses of 6061-T6 aluminum targets. These data were taken at atmospheric pressure, so some (believed minor) air-shock effects cannot be excluded. The upper curve shows the gain in forward momentum derived from flash x-ray measurements of the motion of the remnant target and spall debris (if any—most of this specific data set was obtained with aluminum targets thick enough to prevent spalling, except for the case shown in Fig. 5, with unusually low gain and the points at just over 15 ktap).

The lower curve in Fig. 6 is simply the predicted gain. The effect of the x-ray radiograph line-integral attenuation, including the front edge of target and possible x-ray radiograph nonlinearity, are possible sources of error for cases with spall. The momentum of the incident flyer is calculated from the known (initial) mass/cm$^2$ and the measured flyer velocity. The recoil Kapton mass/cm$^2$ was assumed equal to the initial flyer mass/cm$^2$ , and the recoil velocity of the Kapton was estimated by using the

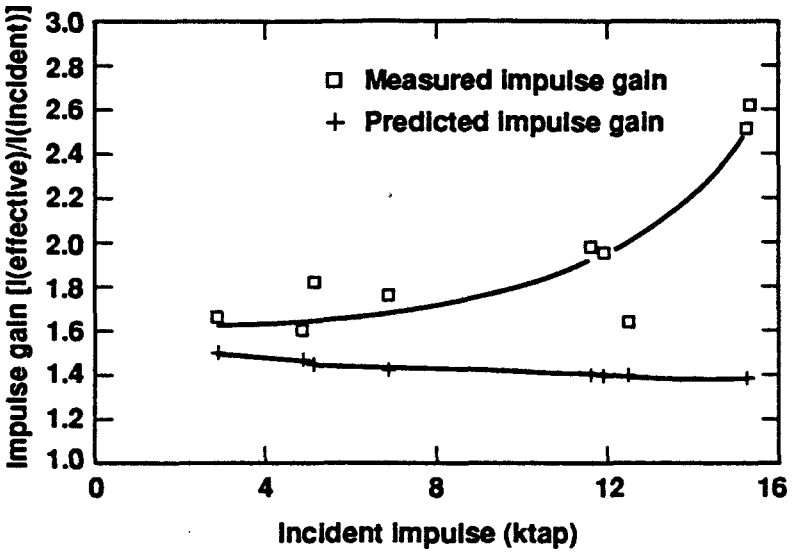


**Figure 6. Measured forward impulse gain from impact of 0.3-mm-thick Kapton flyers at velocities of 0.68 to 3.55 km/s on targets of 6061-T6 aluminum. The incident impulse for a 0.3-mm-thick Kapton flyer (0.043 g/cm$^2$) in ktap is simply 4.3 times the flyer velocity in km/s. The lower curve shown is the gain predicted using the principal Hugoniot for Kapton as an approximation to the release isentrope to calculate the recoil velocity of the Kapton flyer after impact.**

Hugoniot for the Kapton as an approximation to the release isentrope. In the velocity range of the data in Fig. 6, the use of the initial areal mass density appears well justified, as the flyers are generally recovered more or less intact. However, at velocities in excess of about 10 km/s, nothing recognizable as a flyer is recovered, and some erosion of the plasma side of the Kapton flyer is a possibility (we are trying to assess this). Clearly, for the higher velocity range, additional diagnostics or a detailed calculation is needed to evaluate the true input impulse imparted to a target.

We have found that spalling can be predicted rather well in hydrocodes by an instantaneous local stress model. When the tension at a given point in the material reaches a critical value, the material is assumed to fail instantaneously. The previous history of the material is important, of course, as it may affect the value of the critical stress. Failure is not assumed to be affected by local events or conditions, except as they bear on the critical stress at the point.

Equations (1) and (2), which relate the critical stress for spalling to the motion of the rear surface of the spall scab, have been in the literature for some time [5]. F-P measurements made on 6061-T6 aluminum were used with the DYNA2D code to predict the spalling behavior of a matrix of electric-gun shots. Agreement with the experimental measurements of spalling could be obtained only if we increased the critical stress about 50% above the values inferred from the F-P measurements. We have found that the expression for determining the critical stress used the acoustic approximation, in which the release isentrope was treated as a straight line in the pressure-mass velocity plane. With a more realistic representation of the isentrope, the expression became quite a bit more complex, but gave excellent agreement with the values obtained from the DYNA2D runs.

### Attenuation Studies

We have also used the electric gun to measure shock attenuation in silica phenolic and other composite materials. Thin Kapton flyers were accelerated to impact on targets of varying thickness with a diagnostic LiF crystal bonded to their rear surface. An F-P interferometer beam reflected from a spot between the target material and the crystal measured the material velocity of the spot after arrival of the shock wave (and reshock from the target). Such a spot acts as a Lagrangian velocity gauge. Since the Hugoniot of LiF is known accurately, we were able to determine the pressure in the LiF just after reshock. We then used the Hugoniot of the target material to deduce the pressure in the shock wave just before reshock. In Fig. 7 the shock pressure within the LiF crystal is plotted against target thickness for a 0.3-mm-thick Kapton flyer incident at 6 km/s on silicon phenolic targets of various thicknesses backed by an LiF crystal.

Much of the attenuation is determined, of course, by the overtaking rarefaction wave from the back of the flyer, and attenuation versus depth is quite dependent on the thickness of the flyer. For a

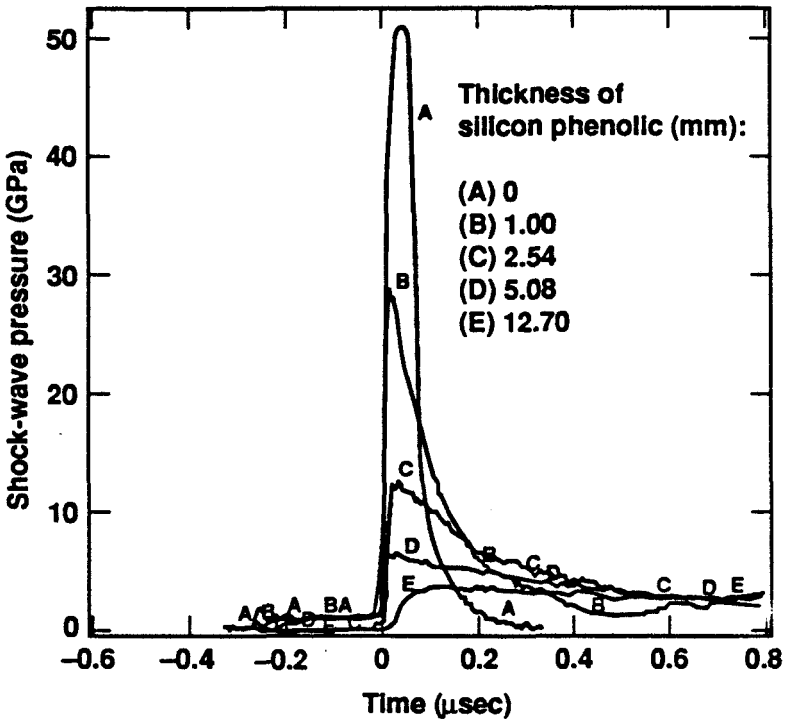


**Figure 7. Shock-wave pressure amplitude vs time for 0.3-mm-thick Kapton flyers impacting at 6 km/s incident on various thicknesses of a silicon phenolic target material. Targets were backed by an LiF diagnostic crystal. Curve A is the reference case, with a bare (aluminum-faced) LiF crystal.**

relatively thick flyer, the overtaking release wave is delayed, and until it reaches the shock, the attenuation is determined essentially by dissipative mechanisms. Thereafter, the decay is dominated by self-similar flow.

### Equation-of-State (EOS) Measurements

We have been developing techniques for making Hugoniot measurements with the electric gun. The advantage over conventional gas-gun or explosive measurements is primarily convenience rather than accuracy. However, it may be possible to extend the technique to impact velocities unreachable by the more conventional methods. Gas guns appear to have reached a flyer velocity limit of about 8 km/s. The highest velocity achieved for an intact flyer with the electric gun is about 20 km/s. The flyer mass was small, but it indicates that one may be able to make Hugoniot measurements at significantly higher velocities and pressures. For example, Froeschner et al. [7] have studied the EOS of tantalum with flyers up to nearly 10 km/s.

The accuracy attainable with the electric gun, however, is not likely to reach that achievable with gas/propellant guns because control over flyer tilt and distortion is limited. Measurements so far have proved most useful for approximate measurements on a material of programmatic interest having rather variable properties. For such materials, the greater precision of gas-gun measurements is not worth the additional cost, since material composition is somewhat inconsistent. We give an example here of a silica phenolic composite material of interest to the space program.

Figure 8 shows the arrangement of our experiment. The target material rests on a common support (outside of the impact area), and is mounted flush with a glass plate having a thin aluminum foil on the bottom to act as a reflector for one beam of an F-P interferometer. This beam serves to signal the time of impact of the flyer (delayed somewhat by the passage of the shock through the aluminum foil). The back of the target is covered with a second aluminum foil of the same thickness to record the arrival time of the shock as indicated by the second beam from the interferometer. The delay in the second foil serves to partially compensate for the delay in the foil under the glass.

The flyer velocity is not directly measured but is inferred from a calibration curve (we have found that the flyer velocity can be predicted within about ±2%). The advantage of this arrangement is that in taking the difference between the arrival times to determine the shock transit time, rise-time delays

caused by the instrument and material response cancel (the same phenomenon is being measured by each beam in a common instrument).

The target density (measured separately) is combined with the experimental shock velocity to form the Rayleigh line, and the Hugoniot of the flyer is reflected and shifted by its velocity to determine the intersection with the principal Hugoniot of the target. Since the flyers we use have unusual Hugoniots (e.g., Kapton requires a cubic fit in the $U_s$ - $U_p$ plane), we have developed special codes for the analysis.

Figure 9 shows the scatter of shots in the $U_s$ - $U_p$ plane. The large scatter is caused by the extremely heterogeneous nature of the target material. The number of fiber filaments included in the target is a function of the thickness.

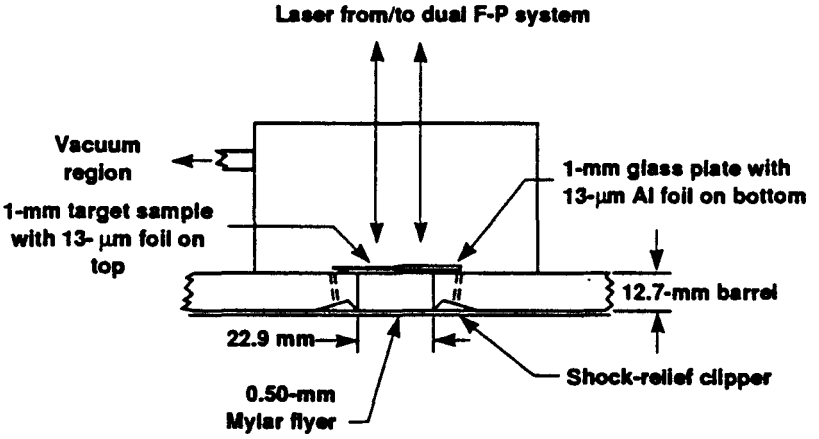


**Figure 8. Experimental setup for EOS measurements on a target material such as silicon phenolic, selected as an example to illustrate work with heterogeneous composite materials.**

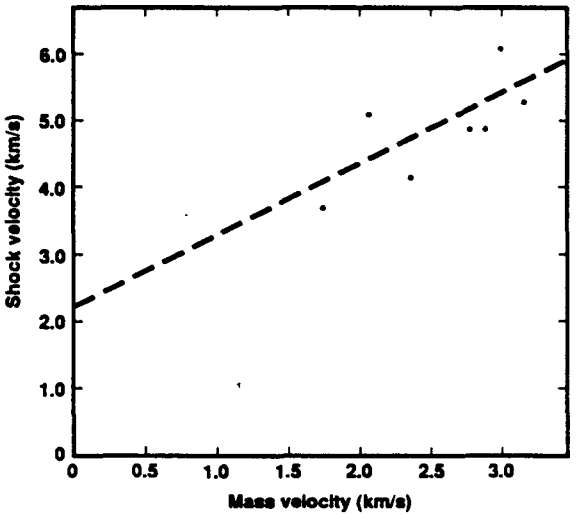


**Figure 9. Best-fit plot of the data on the $U_s$- $U_p$ plane for silicon phenolic targets. The scatter is believed related to the heterogeneous nature of thin samples of material. The plot shows the curve $U_s = 2.209 + 1.087\ U_p$.**

**Reverse-Ballistics Studies**

There is interest in the damage various types of projectiles undergo in penetrating thin walls at hypervelocities. For example, the space program needs to evaluate the best construction and standoff to shield a space station against the impact of most probable and worst types of earth-orbiting or cosmic debris. The electric gun's capability to launch chunky projectiles is limited, but we have demonstrated the capability of launching thin shields or "walls" of dielectric material to impact on well-defined objects initially at rest in the laboratory frame. One series of "reverse-ballistics damage tests used 0.3-mm-thick Kapton flyers impacting at velocities of 11 to 18 km/s on 5-mm-diameter by 19-mm-long rods of different materials and over limited ranges of orientation angle. Early results are described in Ref. [1]. Recent measurements were made with a setup that included a catcher arrangement to measure the angular distribution of impact fragments and melted droplets as well as mass loss from recovered rod tips (typically 10 to 20% of the length of a rod diameter for hard materials such as 4340 armored steel, or loss or complete dispersal of the first centimeter or so for the case of a lead rod).

Our measurements have been made in collaboration with an SRI International group under Don Shockey. Results to be published include an analysis of the mass of the fragments and their crater depths in a soft copper catcher-cylinder. We still cannot independently measure the velocity distribution of each fragment. However, in principle we can also measure the vaporized fraction plated on our catcher walls.

# IV. Summary

The electric gun is capable of launching, intact, thin dielectric flyer plates at velocities as high as 20 km/s. The impact of the flyer generates well-characterized, short-duration, one-dimensional shock waves for use in a wide variety of studies. The examples presented here—spalling and impulse-gain studies, pulse attenuation in composites, EOS measurements in a heterogeneous composites, and a reverse-ballistics study of rod fragmentation—are just a few of the possible applications for this relatively simple and inexpensive tool.

# V. References


1. J. E. Osher, H. H. Chau, G. R. Gathers, R. S. Lee, and R. C. Weingart, "Application of a 100-kV Electric Gun for Hypervelocity Impact Studies," in *Proceedings, 1986 Hypervelocity Impact Symposium*, San Antonio, Texas, October 21–24, 1986.
2. J. Osher, G. Barnes, H. Chau, R. Lee, C. Lee, R. Speer, and R. Weingart, "Operating Characteristics and Modeling of the LLNL 100-kV Electric Gun," submitted to IEEE *Trans. Plasma Sci.* for publication in special June (1989) issue on electromagnetic launchers.
3. C. F. McMillan, D. R. Goosman, N. C. Parker, L. L. Steinmetz, H. H. Chau, T. Huen, R. K. Whipkey, and S. J. Perry, "Velocimetry of Fast Surfaces using Fabry-Perot Interferometry," *Rev. Sci. Instr.* **59**, (1988) pp. 1–20.
4. J. E. Osher, H. H. Chau, G. R. Gathers, R. S. Lee, G. W. Pomykal, and R. C. Weingart, "Shock-Wave Studies Using Plastic Flyers Driven by an Electric Gun for Hypervelocity Impact on Selected Materials," in *Proceedings, 1987 Topical Conference on Shock Waves in Condensed Matter*, Monterey, California, June 20–23, 1987.
5. S. A. Novikov and A. V. Chernov, "Determination of Spall Strength from Measured Values of the Specimen Free-Surface Velocity," *J. Appl. Mech. Tech. Phys.* **5**, 703, (1982).
6. K. E. Froeschner, D. E. Maiden, and H. H. Chau, "Spall Due to Short High-Intensity Impulses," to be published, *J. Appl. Phys.*, April 1989.
7. K. E. Froeschner, R. S. Lee, H. H. Chau, and R. C. Weingart, "Shock Hugoniot Measurements on Ta to 0.78 TPa," in *Shock Waves in Condensed Matter-1983*, (Elsevier Science Publishers, B. V., 1984).